Ultrafast laser ablation of high-voltage cathodes for next generation 3D lithium-ion batteries

Carolyn Reinhold*, Wilhelm Pfleging

Karlsruhe Institute of Technology, Institute for Applied Materials – Applied Materials Physics (IAM-AWP), Hermann-von-Helmholtz-Platz 1, 76344 Eggenstein-Leopoldshafen, Germany

ABSTRACT

A promising approach for enhancing the electrochemical properties of a lithium-ion battery is the combination of a high-voltage cathode with a three-dimensional (3D) electrode architecture created through ultrafast laser ablation. In this work, the ablation characteristics of $LiNi_{0.5}Mn_{1.5}O_4$ (LNMO) cathodes either fabricated by an N-methyl-2-pyrrolidone-based (NMP) or water-based electrode processing were examined. The influence of the binder on the resulting ablation depth as well as the ablation area and volume of the generated grooves was analyzed. An electrochemical analysis of unstructured and selected laser structured LNMO cathodes of both binder types was conducted to characterize the influence of the 3D electrode design on the electrochemical performance. For both LNMO cathodes, a significant increase of the specific discharge capacity at a C-rate of 5C could be observed for the cells containing the laser structured electrode variants.

Keywords: Ultrashort pulsed laser ablation, lithium-ion battery, 3D battery, laser structuring, LNMO

1. INTRODUCTION

The ongoing development of electrifying transportation enhances the demand for affordable, sustainable high-energy and high-power lithium-ion batteries. For reaching this aim, optimized material configurations and electrode architectures are needed. One focus of research is therefore on the use of high-voltage cathodes materials [1, 2]. Among these, especially the high-voltage spinel $LiNi_{0.5}Mn_{1.5}O_4$ (LNMO) is a very promising cathode active material due to its high working potential of 4.7 V and reachable practical capacities of around 140 mAh g^{-1} which results in energy densities around 650 Wh kg^{-1} on material level [2–4]. Advantageous is in addition that the spinel structure provides a three-dimensional network for Li^+ solid state diffusion which facilitates the Li^+ de-/intercalation [3]. Favorable from environmental and cost perspective is furthermore that LNMO, in contrast to NMC, is cobalt-free and uses the nickel redox capacity in its entirety [2]. Another focus of research to improve the environmental aspects as well as the cost-effectiveness of the lithium-ion battery (LIB) production is the implementation of an aqueous electrode processing [5, 6]. State-of-the-art in cathode manufacturing is the use of a polyvinylidene fluoride (PVDF) binder which must be solved in N-methyl-2-pyrrolidone (NMP). Problematic of using NMP is the fact that it is volatile, expensive, and toxic which requires additional ventilation, filtration, and recovery systems to protect the environment and to recover the solvent for reuse [7]. In contrast, aqueous binders are reported to be environmentally friendly, to have lower material prices than PVDF and due to a faster drying process and the fact that no solvent recovery is needed lead to less energy consumption which reduces the battery production costs enormously. [7, 8] An aqueous electrode processing is already successfully implemented in the state-of-the-art anode production where typically a combination of two water-based binders – sodium carboxymethyl cellulose (Na-CMC) and styrene-butadiene rubber (SBR) – is used [5, 6]. However, the realization of a water-based electrode processing for the cathode is not so trivial. Major challenges are the leaching of lithium and transition metal ions from the active material into water and the increase of the pH value which leads to corrosion of the current collector [5, 6]. But nevertheless, the development of an aqueous electrode processing for various cathode materials such as $Li(Ni_xMn_yCo_{1-x-y})O_2$ (NMC), $LiFePO_4$ (LFP) and $LiNi_{0.5}Mn_{1.5}O_4$ (LNMO) using different water-based binders is reported in literature [5, 6]. Besides the materials, also the electrode design plays an important role for achieving high energy and power densities. The 3D battery concept where a three-dimensional surface topography is implemented in the electrode architecture, for example by locally remove electrode material via laser ablation, has been reported to be an effective way to enhance the performance of a LIB by combining the advantageous of the thick-film concept (high mass loading, high energy density) with the benefits of the thin film concept (low ionic resistance, high power density) [9, 10]. The application of this concept has been shown in literature for different cathode and anode materials like LFP [11], NMC [12],

graphite [13], and silicon/graphite [14]. Aim of the ongoing research is now to transfer the 3D battery concept on aqueous processed LNMO electrodes [15].

In the presented work, LNMO cathodes manufactured either by an NMP-based (PVDF binder) or water-based (Na-CMC and fluorinated acrylate polymer latex binder) electrode processing were laser structured using an ultrashort pulsed (USP) laser source. The ablation characteristics of both electrodes were analyzed and compared. The electrochemical properties of corresponding unstructured and selected laser structured LNMO cathodes were evaluated using rate capability measurements.

2. EXPERIMENTAL

2.1 Electrode manufacturing

For the manufacturing of the LNMO cathodes using the NMP-based electrode processing, PVDF powder (Solvay, Germany) was dissolved in NMP (Merck, Germany) with a weight ratio of 1:10 in advance to the slurry fabrication. The LNMO slurry was then prepared by mixing LNMO powder (Haldor Topsoe, Denmark) with conductive carbon black (CB, C-NERGY C65, Imerys G&C, Belgium) in the prepared PVDF solution using a SpeedMixer (DAC 150 SP, Hauschild, Germany). For the aqueous based fabrication of the LNMO cathodes, a water-based 2 wt.% Na-CMC solution (MTI Corporation, USA) was prepared prior to slurry preparation. The LNMO powder was then mixed with CB in the prepared CMC solution using a dissolver (Labor dissolver DB13, DISTECH GmbH, USA). After slurry homogenization, a fluorinated acrylate polymer latex binder TRD 202A (40wt.% solution, JSR Micro NV, Belgium) was stirred into the slurry at a low rotation speed.

Both electrode slurries were casted via doctor blade on an aluminum current collector foil (20 µm thickness) with a universal applicator (ZUA 2000, Proceq, Switzerland) on a film coater (MSK-AFA-III, MTI Corporation, USA). The NMP-based slurry was dried at 90 °C for two hours, whereas the water-based slurry was dried for one hour at 20 °C. Table 1 shows the final composition of both types of LNMO cathode. After drying, the LNMO cathodes were calendered at 20 °C to a porosity of 35 % using an electric rolling presser (MSK-2150, MTI, Cooperation, USA).

Table 1. Composition of LNMO cathodes: NMP-based electrode processing (left,) water-based electrode processing (right)

Material	Mass fraction / wt.%
LNMO	93
C65	4
PVDF	3

Material	Mass fraction / wt.%
LNMO	93
C65	4
TRD 202A	2
Na-CMC	1

2.2 Laser structuring

For the determination of the ablation characteristics of the two different LNMO cathodes, a high-power, high repetition rate laser source (FX600-2-GFH, EdgeWave GmbH, Germany) implemented in a laser material processing system (MSV203 Laser Patterning Tool, M-Solv LTD, United Kingdom) was used. The laser source operates at a wavelength of 1030 nm and has a maximum average laser power P_{avg} of 300 W at a repetition rate f of 1.5 MHz. For the ablation study, three different combinations of repetition rate f and scan speed v, all resulting in the same pulse-to-pulse distance of 13.3 µm leading to line patterns, were utilized (see Table 2). In addition, for all three combinations, six different ratios of average laser power P_{avg} to repetition rate f were applied, chosen in such a way that they result in the same pulse peak fluence E_p for all three variants. Depending on the repetition rate, this means that average laser powers between 1 W and 100 W were applied, leading to pulse peak fluences between 3 J cm^{-2} and 33 J cm^{-2}. The number of laser passes n was varied between 3 and 15. For each parameter set, five lines were created. The generated grooves were analyzed using a digital microscope (VHX 7000, Keyence, Japan). For this, an average profile was created from ten lines with a distance of

10 µm each and the ablation depth, the ablation width at the top as well as the cross-section area of the generated grooves were measured for the five lines.

Table 2. Applied repetition rate and scan speed corresponding to a pulse-to-pulse distance of 13.3 µm.

Repetition rate / kHz	**Scan speed / m s^{-1}**
150	2
750	10
1500	20

2.3 Electrochemical testing

An analysis of the electrochemical properties was conducted on unstructured and structured electrodes of the two different LNMO cathodes with the NMP-based and water-based binder. The structured electrodes were created by applying the parameter set corresponding to the highest aspect ratio. Before cell assembly, the LNMO cathodes were cut in circles with a diameter of 12 mm and dried at 110 °C in a vacuum oven (VT6025, Thermo Scientific, Germany) for 16 hours. Afterwards, CR2032 coin cells were assembled in an argon-filled glovebox (LABmaster pro, M.Braun, Germany) with H_20 < 0.1 ppm and O_2 < 0.1 ppm. A cell consists of an LNMO cathode and a lithium metal anode (0.6 mm thickness, Nanografi, Turkey), a trilayer separator (polypropylene/polyethylene/ polypropylene) (Celgard® 2320, USA) and 120 µl electrolyte (1.3M hexafluorophosphate ($LiPF_6$) dissolved in a mixture of ethylene carbonate (EC) and ethyl methyl carbonate (EMC) with a weight ratio of 3:7 and 5 wt.% fluoroethylene carbonate (FEC)). For the sealing of the cells an electric cell crimper (MSK-160D, MTI Corporation, USA) was used. After cell assembly, the cells were stored for 20 h to ensure complete wetting of all cell components. A constant current – constant voltage (CCCV) protocol for charging and a constant current protocol for discharging were applied by using a battery cycling system (BT 2000, Arbin Instruments, USA) for the formation and subsequent rate capability measurements. Table 3 shows the corresponding C-rates (applied electrical current divided by nominal cell capacity) applied for the different steps. The voltage window for all steps was set to 3.5 V to 4.9 V.

Table 3. C-rates applied for the formation and the rate capability measurement steps.

C-rate for CC charge / h^{-1}	0.05	0.1	0.2	0.5	0.5	0.5	0.5	0.5
C-rate for CV charge / h^{-1}	0.02	0.05	0.05	0.05	0.05	0.05	0.05	0.05
C-rate for CC discharge / h^{-1}	0.05	0.1	0.2	0.5	1	2	3	5
Number of cycles	3	5	5	5	5	5	5	5

3. RESULTS AND DISCUSSION

3.1 Investigation of the ablation characteristics

The ablation characteristics of the LNMO cathodes manufactured either by an NMP-based (PVDF binder) or water-based (Na-CMC and fluorinated acrylate polymer latex binder) electrode processing were studied at three different repetition rates, whereby the ratio of scan speed *v* and repetition rate *f* was kept constant for all applied repetition rates. The resulting ablation depth of the generated grooves in dependence of the pulse peak fluence can be found in Figure 1. For both types of LNMO cathodes, the ablation depth increases with increasing pulse peak fluence for all repetition rates. In addition, both have in common that a lower repetition rate leads to higher ablation depths, especially at higher pulse peak fluence. According to literature, this finding might be caused by shielding effects of the laser-induced vapor/plasma plumes [14]. However, the comparison shows that for the same pulse peak fluence, and repetition rate higher ablation depths can be reached for the LNMO cathode containing the Na-CMC and fluorinated acrylate polymer latex binder. For example, at a pulse peak fluence of 13 J cm^{-2} and a repetition rate of 150 kHz, an average ablation depth of 35 µm can be

reached for the LNMO cathode containing the PVDF binder, whereas the average ablation depth of the LNMO cathode with the Na-CMC and fluorinated acrylate polymer latex binder is 58 µm.

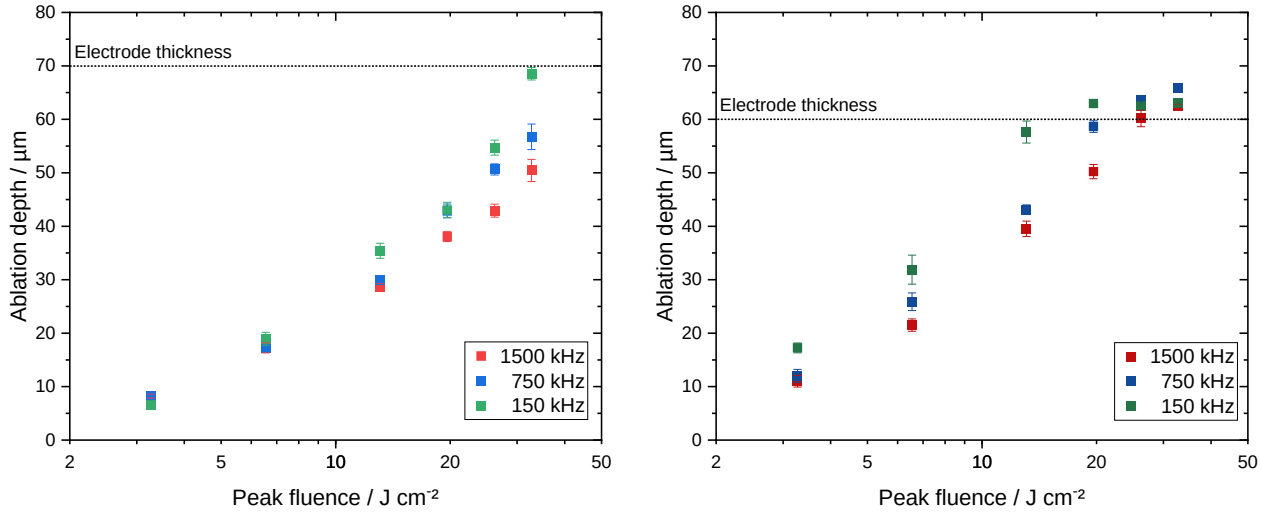

Figure 1. Ablation depth of the LNMO cathode with the NMP-based binder (left) and the water-based binders (right) depending on the pulse peak fluence E_p for different repetition rates (number of laser passes n =9).

A characterization of the total amount of ablated electrode material during the laser structuring for each parameter set is done by calculating the ablation area (cross-section area of generated grooves) and the associated volume. The ablation area and the corresponding ablation volume are shown in Figure 2. An increase of the ablation area and volume can be observed with an increase of the pulse peak fluence for both LNMO cathode types as well. But also in this case, for the LNMO cathodes containing the Na-CMC and fluorinated acrylate polymer latex binder, the ablation area and volume is significantly higher than for the ones with the PVDF binder at a similar pulse peak fluence, e.g., 1562 µm^2 (f = 150 kHz, E_p = 13 J cm^{-2}) compared to 872 µm^2 (f = 150 kHz, E_p = 13 J cm^{-2}).

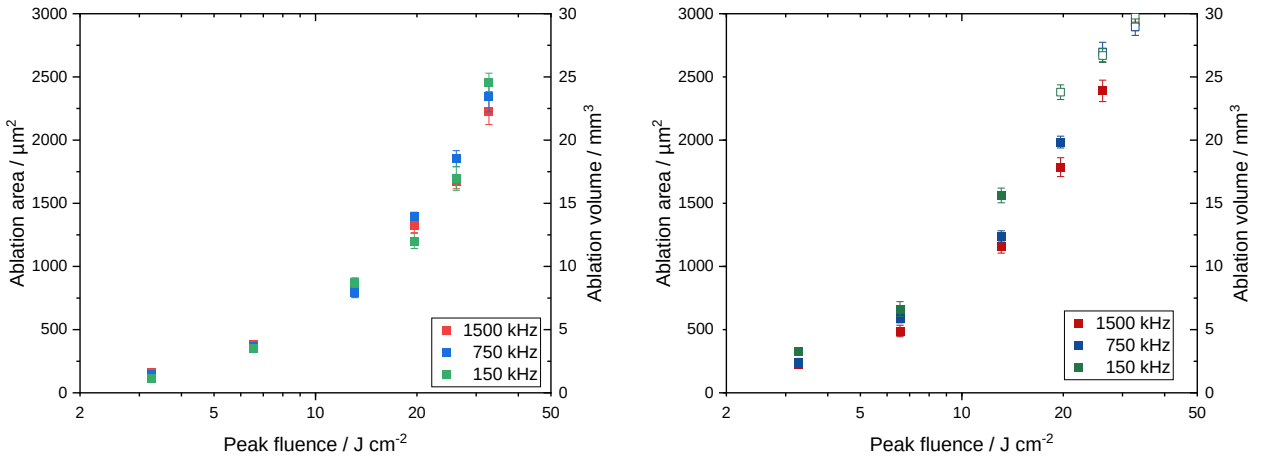

Figure 2. Ablation area and associated volume of the LNMO cathode with the NMP-based binder (left) and the water-based binders (right) depending on the pulse peak fluence E_p for different repetition rates (number of laser passes n = 9). Solid symbols: aluminum current collector was not exposed; open symbols: aluminum current collector exposed.

The results indicate that the dominating ablation mechanism for the LNMO cathodes seems to be the binder decomposition and the subsequent ejection of LNMO particles in which the decomposition temperature of the binder determines the amount of electrode material that can be ablated at a defined pulse peak fluence. The temperatures of the decomposition range of Na-CMC are with 220 to 410 °C [16] (maximum degradation rate at around 290 °C [16, 17]) significantly lower than the PVDF decomposition range of 350 to 600 °C [18] (maximum decomposition rate at around 492 °C [19, 20]), thus, more electrode material can be ablated for the LNMO cathode containing the combination of Na-CMC and TRD 202A as a binder. Therefore, for this LNMO cathode either less number of laser passes are needed to expose the aluminum current collector as for the LNMO cathode containing the PVDF binder at a similar pulse peak fluence and electrode thickness or a lower pulse peak fluence can be applied for the same number of laser passes and electrode thickness as for the LNMO cathode containing the PVDF binder.

3.2 Electrochemical analyses

A characterization of the electrochemical properties of unstructured and structured LNMO cathodes for both types, containing NMP-based PVDF binder or water-based Na-CMC and fluorinated acrylate polymer latex binder, was conducted by rate capability measurements. The average specific discharge capacities of the LNMO cathodes as a function of the applied C-rate are shown in Figure 3. For both types of LNMO cathodes, the same trend can be identified. At low C-rates (C/10 till C/2), nearly the same specific discharge capacities could be achieved, varying between 133 mAh g^{-1} and 139 mAh g^{-1}. If the C-rate is further increased (till 5C), a decrease of the reachable discharge capacity could be observed. However, the cells containing the laser structured electrodes showed a less pronounced decrease compared with the cells containing the unstructured ones. For example, at a C-rate of 5C, the average specific discharge capacity could be increased from 33 mAh g^{-1} to 98 mAh g^{-1} for the cells containing the LNMO cathode with the PVDF binder, whereas it could be increased from 42 mAh g^{-1} to 112 mAh g^{-1} for the cells containing the LNMO cathode with Na-CMC and TRD 202A as a binder. This corresponds to an increase of 296 % for the first or of 266 % for the latter. All in all, slightly higher discharge capacities ccould be observed for the cells containing the LNMO cathode with the Na-CMC and fluorinated acrylate polymer latex binder.

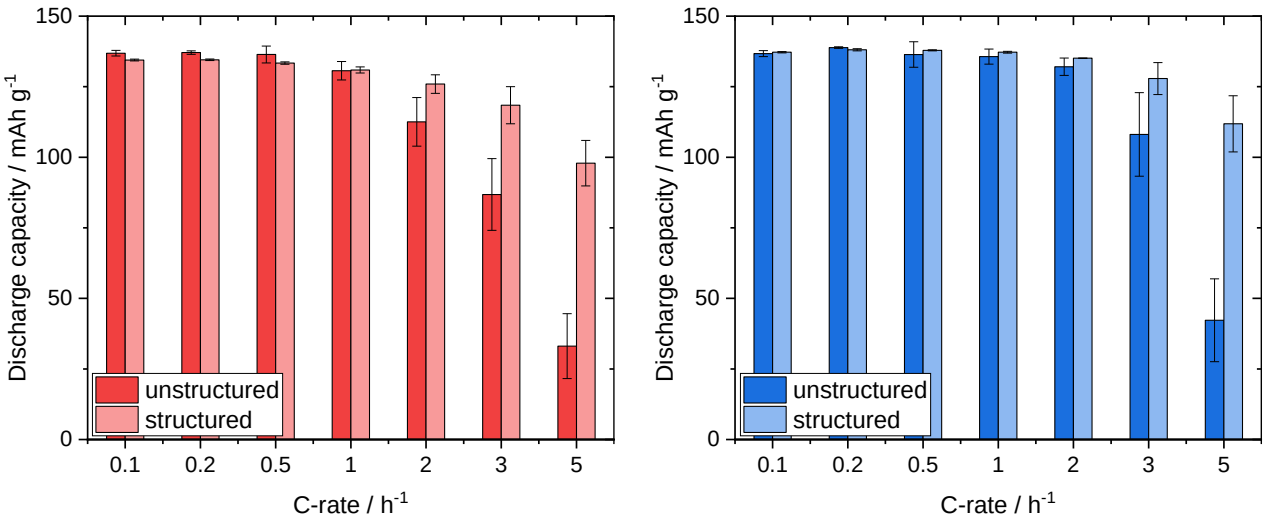

Figure 3. Rate capability measurements of cells containing unstructured and structured LNMO cathodes with NMP-based PVDF binder (left) and water-based Na-CMC and fluorinated acrylate polymer latex binder (right).

Responsible for the enhancement of the specific discharge capacities at higher C-rate for the laser structured LNMO cathode variants are the improved Li^+ diffusion kinetics. With the local ablation of electrode material, additional electrode surfaces are created, shortening the Li^+ diffusion pathways inside the porous electrode structure and thus minimizing the Li^+ concentration gradient. Consequently, the overall cell polarization is reduced, allowing high discharge capacities even at higher C-rates.

4. CONCLUSION

In the presented work, the influence of two different binder systems on the ablation characteristics of LNMO cathodes were analyzed. In addition, the impact of a line structure patterning on the electrochemical performance for these electrodes was evaluated. Therefore, LNMO cathodes manufactured either by an NMP-based (PVDF binder) or water-based (Na-CMC and fluorinated acrylate polymer latex binder) electrode processing were laser structured using an USP laser source. For the analysis of the ablation behavior, the repetition rate and pulse peak fluence were varied while keeping a constant pulse-to-pulse distance. For both types of LNMO cathodes, a dependency of the ablation depth and the ablation area/volume on the repetition rate and pulse peak fluence could be observed. However, higher values were reached for the LNMO cathode containing Na-CMC and TRD202A as a binder which could be attributed to the lower decomposition temperature of CMC. An analysis of the electrochemical performance for unstructured and selected laser structured LNMO cathodes for both cathode types was conducted in coin cells versus lithium. Rate capability measurements demonstrated that the implementation of a line structure patterning could increase the reachable specific discharge capacities of both LNMO cathodes significantly, especially at high C-rates.

ACKNOWLEDGEMENT

This project receives funding from the European Union's Horizon Europe research and innovation program under grant agreement no. 101069508 (HighSpin).

REFERENCES

[1] Booth, S. et al. 2021. "Perspectives for next generation lithium-ion battery cathode materials". *APL Materials*. DOI: 10.1063/5.0051092.

[2] Stüble, P. et al. 2023. "On the composition of $LiNi_{0.5}Mn_{1.5}O_4$ cathode active materials". *Advanced Energy Materials*. DOI: 10.1002/aenm.202203778.

[3] Fehse, M. et al. 2022. "Influence of transition-metal order on the reaction mechanism of LNMO cathode spinel: An operando X-ray absorption spectroscopy study". *Chemistry of materials: a publication of the American Chemical Society*. DOI: 10.1021/acs.chemmater.2c01360.

[4] Armand, M. et al. 2020. "Lithium-ion batteries – Current state of the art and anticipated developments". *Journal of Power Sources*. DOI: 10.1016/j.jpowsour.2020.228708.

[5] Bresser, D. et al. 2018. "Alternative binders for sustainable electrochemical energy storage – the transition to aqueous electrode processing and bio-derived polymers". *Energy & Environmental Science*. DOI: 10.1039/C8EE00640G.

[6] Pillai, A. et al. 2022. "Aqueous binders for cathodes: a lodestar for greener lithium-ion cells". *Energy & Fuels*. DOI: 10.1021/acs.energyfuels.2c00346.

[7] Wood, D. et al. 2015. "Prospects for reducing the processing cost of lithium-ion batteries". *Journal of Power Sources*. DOI: 10.1016/j.jpowsour.2014.11.019.

[8] Susarla, N. et al. 2018. "Modeling and analysis of solvent removal during Li-ion battery electrode drying". *Journal of Power Sources*. DOI: 10.1016/j.jpowsour.2018.01.007.

[9] Pfleging, W. 2022 - 2022. "3D electrode architectures for high energy and high power lithium-ion batteries. In: Balaya, P. et al. [Editors] *Energy Harvesting and Storage: Materials, Devices, and Applications XII*. SPIE. 2. DOI: 10.1117/12.2623655.

[10] Pfleging, W. 2021. "Recent progress in laser texturing of battery materials: a review of tuning electrochemical performances, related material development, and prospects for large-scale manufacturing". *International Journal of Extreme Manufacturing*. DOI: 10.1088/2631-7990/abca84.

[11] Mangang, M. et al. 2014. "Ultrafast laser microstructuring of $LiFePO_4$ cathode material. In: Klotzbach, U. et al. [Editors] *Laser-based Micro- and Nanoprocessing VIII*. SPIE. 89680M. DOI: 10.1117/12.2039604.

[12] Song, Z. et al. 2021. "Electrochemical performance of thick-film $Li(Ni_{0.6}Mn_{0.2}Co_{0.2})O_2$ Cathode with Hierarchic Structures and Laser Ablation". *Nanomaterials*. DOI: 10.3390/nano11112962.

[13] Jan Bernd Habedank. 2021. *Laser Structuring of Graphite Anodes for Functionally Enhanced Lithium-Ion Batteries.* Dissertation. München.

[14] Meyer, A. et al. 2023. "High repetition ultrafast laser ablation of graphite and silicon/graphite composite electrodes for lithium-ion batteries". *Journal of Laser Applications*. DOI: 10.2351/7.0001180.

[15] European commission. 2022. *High-Voltage Spinel LNMO Silicon-Graphite Cells and Modules for Automotive and Aeronautic Transport Applications [online].* See https://cordis.europa.eu/project/id/101069508.

[16] Trevisol, T. et al. 2019. "Alginate and carboxymethyl cellulose in monolayer and bilayer films as wound dressings: Effect of the polymer ratio". *Journal of Applied Polymer Science*. DOI: 10.1002/app.46941.

[17] Tan, L. et al. 2017. "Effect of Na^+ and Ca^{2+} on the Thermal Degradation of Carboxymethylcellulose in Air". *Polymers and Polymer Composites*. DOI: 10.1177/096739111702500408.

[18] Rensmo, A. et al. 2023. "Lithium-ion battery recycling: a source of per- and polyfluoroalkyl substances (PFAS) to the environment?". *Environmental science. Processes & impacts*. DOI: 10.1039/D2EM00511E.

[19] Jie, Y. et al. 2020. "Waste organic compounds thermal treatment and valuable cathode materials recovery from spent $LiFePO_4$ batteries by vacuum pyrolysis". *ACS Sustainable Chemistry & Engineering*. DOI: 10.1021/acssuschemeng.0c07424.

[20] Swann, J. und Stoliarov, S. 2021. "Determination of pyrolysis and combustion properties of poly(vinylidene fluoride) using comprehensive modeling: Relating heat transfer to the intumescent char's porous structure". *Fire Safety Journal*. DOI: 10.1016/j.firesaf.2020.103086.